Inorganic Chemistry

Article

pubs.acs.org/IC

Synthesis, Characterization, and Luminescence Studies of Discrete Polynuclear Gold(I) Sulfido and Selenido Complexes with Intramolecular Aurophilic Contacts

Eddie Chung-Chin Cheng, Wing-Yin Lo, Terence Kwok-Ming Lee, Nianyong Zhu, and Vivian Wing-Wah Yam*

Institute of Molecular Functional Materials [Areas of Excellence Scheme, University Grants Committee (Hong Kong)], and Department of Chemistry, The University of Hong Kong, Pokfulam Road, Hong Kong, PR China

Ⓢ *Supporting Information*

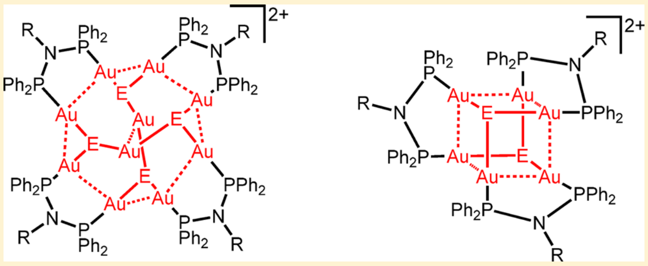

ABSTRACT: The synthesis, characterization, and photophysical and photochemical properties of a family of high-nuclearity gold(I) chalcogenides, specifically, the gold(I) sulfido and selenido complexes containing different bridging diphosphine ligands with nuclearities of ten ($[Au_{10}\{\mu\text{-}Ph_2PN(R)PPh_2\}_4(\mu_3\text{-}E)_4]^{2+}$) and six ($[Au_6\{\mu\text{-}Ph_2PN(R)PPh_2\}_3(\mu_3\text{-}E)_2]^{2+}$), are reported. The X-ray crystal structures of the complex cations of Au_{10} and Au_6 are found to be propeller-like structures and distorted cubane structures, respectively, with the presence of short intramolecular gold···gold distances. The complexes show intense green and/or orange phosphorescence upon photoexcitation in the solid state and in solution at ambient and low temperature. The emission properties are found to be strongly dependent on the nuclearities and the chalcogenido ligands, but are rather insensitive to the substituents on the bis(diphenylphosphino)amines. The emissions are tentatively assigned to originate from the excited states derived from the phosphine-centered intraligand (IL) transition or metal-centered (ds/dp) mixed with ligand-to-metal–metal charge transfer (LMMCT) (E→Au) transition. The photochemical properties of the complexes were also studied by transient absorption spectroscopy.

■ INTRODUCTION

Metal chalcogenides with d^{10} electronic configuration have been widely used as photovoltaic semiconductor materials and photocatalysts.[1] Most of them are also known to exhibit interesting optical properties, depending on the size of the particles (quantum-size effect).[2] Indeed, soluble polynuclear d^{10} metal chalcogenides and chalcogenolates are especially interesting in that they may serve as model systems for the study and understanding of metal chalcogenides, which have been widely used as photovoltaic semiconductor materials and photocatalysts as well as thiolate monolayer protected clusters (MPC) of noble metals, especially those of gold.[1] Besides, the chemistry of transition metal chalcogenides and chalcogenolates represents a very important division of structural chemistry owing to the highly flexible bonding modes of the chalcogen-containing ligands. Numerous polynuclear copper(I) and silver(I) chalcogenido clusters, with monodentate and bidentate phosphine ligands as protective ligand shells, have been reported.[3] With the variation of solvents, anions, and substituents on the phosphines and chalcogenido-silanes, which are widely employed as precursors of chalcogenides, different nuclearities and structures can be obtained, and their luminescence and photoredox properties can be fine-tuned.

Apart from these chalcogenido complexes of the lighter congeners, polynuclear gold(I) chalcogenides have also attracted increasing attention,[4] despite the fact that not only is the coordination chemistry of monovalent gold more restricted but also that the preparation of them is complicated by the tendency to form insoluble binary chalcogenides or polymeric materials.[4d] These problems have been circumvented or avoided by stabilization with phosphine ligands.[4,5] However, examples involving the use of the bridging phosphine ligands for constructing high-nuclearity clusters are relatively less explored.[4,6,7] In particular, the exhaustive studies on their luminescence properties are relatively rare,[4e,7] although other types of gold(I) cluster systems were recently shown to be intensely luminescent.[8,9] While soluble polynuclear gold(I) sulfido complexes are already very rare,[7b,c] even more scarce are their selenido analogues.[7f] As an extension of our earlier reports on luminescent polynuclear gold(I) sulfido complexes,[7a−c,e] herein we report the synthesis, characterization, and photophysical and photochemical studies of a series of decanuclear and hexanuclear gold(I) sulfido and its heavier congener, selenido complexes, $[Au_{10}\{\mu\text{-}Ph_2PN(R)PPh_2\}_4(\mu_3\text{-}E)_4](X)_2$ (where E = S, X = PF_6, R = ^{n}Pr (**1**);[7b] E = S, X = ClO_4, R = C_6H_5 (**2**), $C_6H_4CH_3$-*p* (**3**), $C_6H_4OCH_3$-*p* (**4**), C_6H_4Cl-*p* (**5**), C_6H_4Br-*p* (**6**) and C_6H_4F-*p* (**7**); E = Se, X = ClO_4, R = ^{n}Pr (**8**),

Received: January 28, 2014
Published: March 12, 2014

Ph (**9**), C_6H_4Me-*p* (**10**), and C_6H_4F-*p* (**11**)) and $[Au_6\{\mu\text{-}Ph_2PN(R)PPh_2\}_3(\mu_3\text{-}E)_2](X)_2$ (where E = S, X = PF_6, R = ^{n}Pr (**12**); E = S, X = ClO_4, C_6H_5 (**13**), $C_6H_4CH_3$-*p* (**14**),[7c] and $C_6H_4OCH_3$-*p* (**15**); E = Se, X = PF_6, R = ^{n}Pr (**16**); E = Se, X = ClO_4, R = Ph (**17**), and C_6H_4Me-*p* (**18**); and E = Se, X = PF_6, R = C_6H_4F-*p* (**19**)) (Chart 1). The single-crystal structures of five of the gold(I) clusters have been determined, and extensive intramolecular aurophilic contacts have been observed.

Chart 1. Schematic Drawings of the Cations of the Gold(I) Sulfido and Selenido Complexes

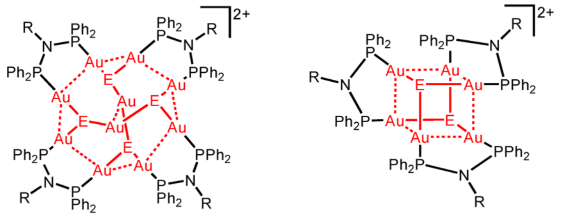

E = S, R = ^{n}Pr (**1**), C_6H_5 (**2**), $C_6H_4CH_3$-*p* (**3**), $C_6H_4OCH_3$-*p* (**4**), C_6H_4Cl-*p* (**5**), C_6H_4Br-*p* (**6**) and C_6H_4F-*p* (**7**)

E = Se, R = ^{n}Pr (**8**), C_6H_5 (**9**), $C_6H_4CH_3$-*p* (**10**), and C_6H_4F-*p* (**11**)

E = S, R = ^{n}Pr (**12**), C_6H_5 (**13**), $C_6H_4CH_3$-*p* (**14**) and $C_6H_4OCH_3$-*p* (**15**),

E = Se, R = ^{n}Pr (**16**), C_6H_5 (**17**), $C_6H_4CH_3$-*p* (**18**), and C_6H_4F-*p* (**19**)

■ RESULTS AND DISCUSSION

Synthesis. The synthesis and isolation of polynuclear gold(I) sulfido complexes with various bridging bis(diphenylphosphino)amine ligands were successfully achieved in the presence of air. Reaction of $[Au_2\{\mu\text{-}Ph_2PN(R)PPh_2\}Cl_2]$ (where R = ^{n}Pr, C_6H_5, $C_6H_4CH_3$-*p*, $C_6H_4OCH_3$-*p*, C_6H_4Cl-*p*, C_6H_4Br-*p*, or C_6H_4F-*p*) in an ethanol/pyridine mixture with H_2S, followed by the metathesis reaction with either NH_4PF_6 or $LiClO_4{\cdot}3H_2O$, gave simultaneously the decanuclear and hexanuclear gold(I) complexes $[Au_{10}\{\mu\text{-}Ph_2PN(R)PPh_2\}_4(\mu_3\text{-}S)_4]^{2+}$ and $[Au_6\{\mu\text{-}Ph_2PN(R)PPh_2\}_3(\mu_3\text{-}S)_2]^{2+}$ in their corresponding salts. In the synthetic procedure, H_2S was preferred over Na_2S because the latter would generate an impure mixture and thus result in a lower yield. Apart from the use of H_2S or Na_2S, the use of $E(SiMe_3)_2$ and $RESiMe_3$ has also been commonly reported for the preparation of other metal chalcogenido clusters.[10] Pyridine was carefully chosen to act as a mild base to deprotonate H_2S, forming the nonreacting pyridinium chloride and at the same time keeping the reaction condition as mild as possible to enhance the stability of the labile d^{10} metal complex in the reaction mixture. This is important as the soft gold(I) ion would tend to form complexes with the soft sulfide ligands rather than the hard nitrogen-containing ligands such as pyridine. This would somehow stabilize the transition state of the reaction intermediate and favor the formation of the target complex. The use of strong bases such as KOH was not preferred, as an aqueous medium would be required, which may cause decomposition of the labile gold(I) precursor complex or the final target complex. However, the controlled isolation of one complex over the other as the major product was difficult and could not be readily achieved, and in most cases mixtures of both the decanuclear and hexanuclear gold(I) complexes were isolated. In some cases, only the decanuclear complexes were isolated, and attempts to isolate the hexanuclear complexes were not successful. Also, because the decanuclear and the hexanuclear complexes possess very similar solubilities and properties in common organic solvents, the isolation and separation of the two complexes were only achieved by the repeated recrystallization and mechanical separation.

The synthesis of a series of analogous gold(I) selenido clusters was also pursued, which gave rise to the successful isolation of the desired products. The syntheses of hexanuclear and decanuclear gold(I) selenido clusters were attempted by the one-pot reaction of dinuclear gold(I) chloride precursors $[Au_2\{\mu\text{-}Ph_2PN(R)PPh_2\}Cl_2]$ (R = ^{n}Pr, Ph, C_6H_4Me-*p*, and C_6H_4F-*p*) with Na_2Se in CH_2Cl_2 under anhydrous and anaerobic conditions. The reaction mixture was allowed to stir for 2 d to ensure a complete reaction. The metathesis reaction with either NH_4PF_6 or $LiClO_4$ gave $[Au_{10}\{\mu\text{-}Ph_2PN(R)PPh_2\}_4(\mu_3\text{-}Se)_4]^{2+}$ and $[Au_6\{\mu\text{-}Ph_2PN(R)PPh_2\}_3(\mu_3\text{-}Se)_2]^{2+}$ in their corresponding salts. Note that the gold(I) selenido system required preparation under an inert atmosphere because of the high tendency of selenido species to form polyselenide mixtures in air, and this would lead to a mixture of products. The high nuclearity gold(I) complexes are believed to be formed upon their reaction with the chalcogenido ligands, rather than after the addition of NH_4PF_6 or $LiClO_4$, based on the following grounds. First, intense photoluminescence could be observed (though weaker than that for the final complexes with the noncoordinating counter-anions) during the course of the reaction, especially after the removal of the reaction solvent. Such photoluminescence was characteristic of the high nuclearity gold(I) chalcogenido clusters; for example, both green-emitting and orange-emitting solids could be observed for the sulfido complexes. Furthermore, the preferred 2-coordinate geometry of the gold(I) centers, the relative stronger Au−P and Au−S/Se bonds over the Au−Cl bond, as well as the noncoordinating nature of the PF_6^- and ClO_4^- anions all support the assignment that the clusters were formed in situ during the reaction with chalcogenides rather than during the metathesis reaction.

Crystal Structure Determination. *Decanuclear Gold(I) Complexes.* The perspective drawings of the decanuclear gold(I) complex cations of **3**, **5**, and **8** with atomic numbering are shown in Figure 1 and Supporting Information, Figures S1 and S2, respectively. The crystallographic data and the average bond lengths and distances are given in Supporting Information, Tables S1−S6. The complex cations possess a propeller-like structure with four $PNP\text{-}Au_2$ units linked together by four sulfur or selenium atoms. The opposite pairs of sulfur or selenium atoms are bonded to the two gold atoms at the core in a linear fashion. An S_4 symmetry axis passes through these two central gold atoms and gives rise to an S_4 point group. Significant intramolecular Au(I)···Au(I) interactions exist (Au(I)···Au(I) distances = 3.0387(16)−3.2240(8) Å for **3**, 3.0538(6)−3.2119(7) Å for **5**, and 3.0184(12)−3.1777(10) Å for **8**). These values are comparable to those observed in common gold(I) chalcogenido complexes such as $[Au\{S(AuPPh_3)_2\}_2][(CH_3)_3SnCl_2]$ (3.030−3.213 Å),[11] $[Au_{10}Se_4(dppm)_4]^{2+}$ (3.061−3.363 Å),[6f] $[Au_{12}(\mu\text{-}dppm)_6(\mu_3\text{-}S)_4]^{2+}$ (3.001−3.342 Å),[7a] and **1** (3.0255−3.2783 Å).[7b] The Au−S (ca. 2.314−2.334 Å) and Au−Se (2.420−2.446 Å) bond lengths are typical of those found in other gold(I) μ_3-sulfido[12] and μ_3-selenido[6e,f] complexes, respectively. The Au−Se bond distances are generally slightly longer than the Au−S distances in the related decanuclear gold(I) sulfido clusters,[7b] in accord with the larger size of the selenium atoms over the sulfur atoms.

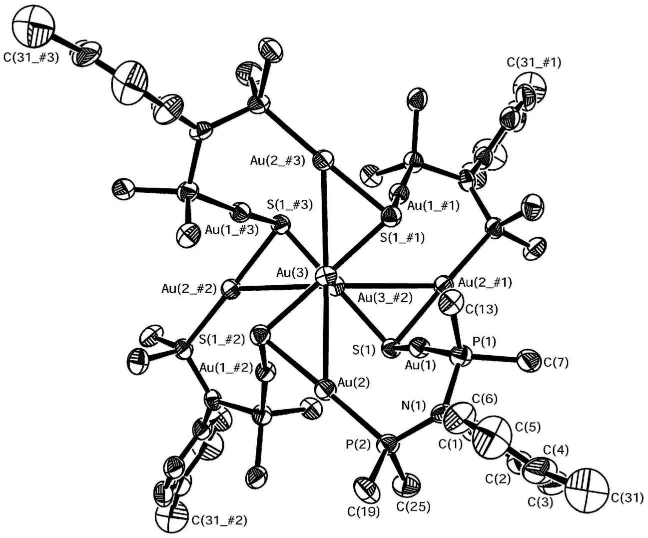

Figure 1. Perspective drawing of the complex cation of **3** with the atomic numbering scheme. Only the *ipso*-carbons of the phenyl rings that are bonded to the phosphorus atoms are shown, and hydrogen atoms have been omitted for clarity. Thermal ellipsoids are shown at the 30% probability level.

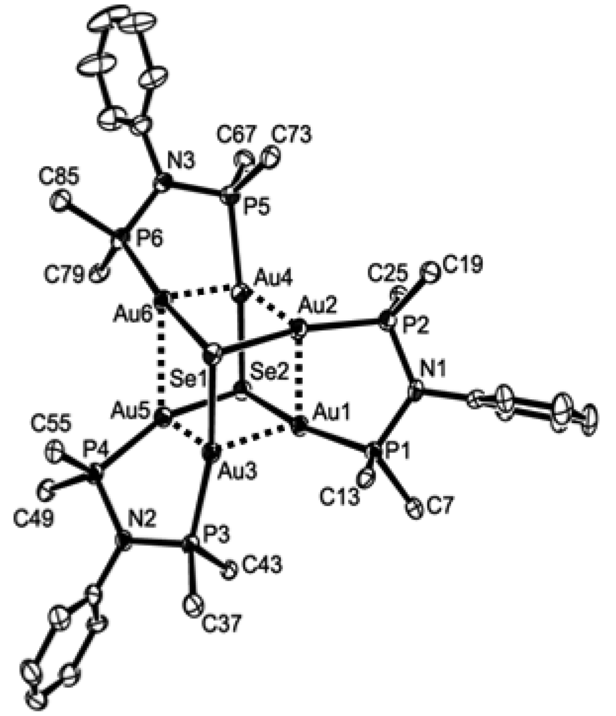

Figure 2. Perspective drawing of the complex cation of **17** with the atomic numbering scheme. Only the *ipso*-carbons of the phenyl rings that are bonded to the phosphorus atoms are shown, and hydrogen atoms have been omitted for clarity. Thermal ellipsoids are shown at the 30% probability level.

Each gold(I) atom is coordinated to a phosphorus and a chalcogen atom, and the coordination is distorted from that of an ideal linear geometry. The Au−S−Au and Au−Se−Au angles are found to deviate from 90° and are in the range of 78.52(5)−103.189(14)°. The coordination geometry about the nitrogen atom of the bis(phosphino)amine ligand is almost trigonal planar, with P−N−P angles having a value very close to 120°. Such a planar geometry is commonly found in compounds involving this class of ligands.[13]

Hexanuclear Gold(I) Complexes. The X-ray crystal structures of **16** and **17** were obtained, showing that they are hexanuclear in nature, having distorted cubane structures, and the two selenium atoms are at opposite apexes, which are similar to those of the sulfido analogue **14**.[7c] Figure 2 and Supporting Information, Figure S3 depict the perspective drawings of the complex cations of **17** and **16**, respectively, and Supporting Information, Tables S7−S10 summarize the crystal structure determination data and selected bond lengths and bond angles. Each selenium atom is bonded to three gold(I) centers in a μ_3-bridging mode, and the two $\mathrm{Au_3Se}$ units are interconnected by three $\mathrm{Ph_2PN(R)PPh_2}$ ligands. A C_3 symmetry axis passes through the two selenium atoms, with three perpendicular C_2 axes each bisecting the phosphine ligands to give rise to a D_3 point group. Noticeable Au(I)···Au(I) interactions are observed, and the Au(I)···Au(I) distances range from 2.9264(7) to 3.3508(10) Å. The Au−Se and Au−P bond distances of 2.4250(11)−2.4453(11) Å and 2.272(3)−2.288(3) Å, respectively, and the Au−Se−Au angles of 87.00(4)−95.80(4)° that are deviated from the ideal value of 90°, are commonly observed in gold(I) μ_3-selenido complexes.[6e,f] Similar to **1**,[7b] **3**, **5**, **8**, and **14**,[7c] the P−N−P angles are very close to 120°, indicative of a sp^2 hybridization at the N center.

Electronic Absorption Spectroscopy. The electronic absorption data for $[\mathrm{Au_{10}}\{\mu\text{-}\mathrm{Ph_2PN(R)PPh_2}\}_4(\mu_3\text{-E})_4]^{2+}$ (**2**−**11**) and $[\mathrm{Au_6}\{\mu\text{-}\mathrm{Ph_2PN(R)PPh_2}\}_3(\mu_3\text{-E})_2]^{2+}$ (**12**, **13**, **15**−**19**) in dichloromethane at 298 K are summarized in Table 1. All of them show similar absorption patterns, with an intense high-energy absorption shoulder at ca. 262−273 nm, a lower-energy absorption shoulder at ca. 304−344 nm, and a low-energy absorption band at ca. 344−439 nm, resembling those of **1**[7b] and **14**.[7c] The high-energy absorptions in the UV region, which are also found in the spectra of the corresponding $\mathrm{Ph_2PN(R)PPh_2}$ ligand and the gold(I) precursor complex, $[\mathrm{Au_2}\{\mu\text{-}\mathrm{Ph_2PN(R)PPh_2}\}\mathrm{Cl_2}]$, are assigned to an intraligand transition or a metal-perturbed intraligand transition.[7b,c] The low-energy absorption shoulders, which are absent in the gold(I) precursor complexes $[\mathrm{Au_2}\{\mu\text{-}\mathrm{Ph_2PN(R)PPh_2}\}\mathrm{Cl_2}]$ are likely to originate from a ligand-to-metal charge-transfer transition modified by Au···Au interactions (LMMCT; E→Au).[7b,c]

Luminescence Properties. *Decanuclear Gold(I) Complexes.* Excitation of the decanuclear complexes in the solid state and in solution with visible light at $\lambda \geq 400$ nm at room temperature and at 77 K results in intense dual luminescence in the green and orange-red region. Table 2 summarizes the luminescence data of the decanuclear gold(I) complexes **2**−**11**, and Figure 3 illustrates the emission spectrum of **2** in the solid state at 77 K. The radiative lifetimes in the microsecond range are suggestive of a triplet parentage. The high-energy emission in the green region with a comparatively shorter lifetime (in the solid state) is attributed to the metal-perturbed ligand-centered phosphorescence, while the low-energy emission in the orange-red region is assigned to originate from the triplet states of a ligand-to-metal charge-transfer character that mixed with metal-centered (ds/dp) states modified by Au···Au interactions (LMMCT; E→Au), as suggested in the previous study of **1**.[7b] The assignment is further supported by the fact that the low-energy emission of the selenido analogues is red-shifted when compared to the sulfido counterparts (Table 2), given the more electron-rich nature of the selenido ligand. In addition,

Table 1. Electronic Absorption Data for $[Au_{10}\{\mu\text{-}Ph_2PN(R)PPh_2\}_4(\mu_3\text{-}E)_4]^{2+}$ (1−11) and $[Au_6\{\mu\text{-}Ph_2PN(R)PPh_2\}_3(\mu_3\text{-}E)_2]^{2+}$ (12−19) in Dichloromethane at 298 K

complex	R	E	λ_{max}/nm (ε/dm^3 mol^{-1} cm^{-1})
1	^{n}Pr	S	268 sh (71 620), 336 sh (24 920), 400 (3930)
2	C_6H_5	S	266 sh (100 550), 326 sh (33 470), 418 (4120)
3	C_6H_4Me-*p*	S	262 sh (113 030), 326 sh (34 800), 418 (4210)
4	C_6H_4OMe-*p*	S	270 sh (119 350), 330 sh (36 190), 416 (4320)
5	C_6H_4Cl-*p*	S	262 sh (121 010), 328 sh (34 810), 416 (3640)
6	C_6H_4Br-*p*	S	326 sh (35 260), 418 (4100)
7	C_6H_4F-*p*	S	262 sh (104 910), 326 sh (33 670), 418 (3760)
8	^{n}Pr	Se	270 sh (130 010), 326 sh (37 460), 426 (3710)
9	C_6H_5	Se	271 sh (101 330), 344 sh (26 410), 439 (3250)
10	C_6H_4Me-*p*	Se	273 sh (93 460), 344 sh (24 560), 433 (3150)
11	C_6H_4F-*p*	Se	267 sh (98 220), 340 sh (28 280), 437 (3280)
12	^{n}Pr	S	260 sh (72 360), 304 (24 140), 348 (6480)
13	C_6H_5	S	264 sh (74 590), 304 sh (23 160), 346 (6420)
14	C_6H_4Me-*p*	S	264 sh (83 280), 304 sh (24 290), 346 (6320)
15	C_6H_4OMe-*p*	S	266 sh (92 160), 306 sh (23 510), 344 (6430)
16	^{n}Pr	Se	269 sh (59 710), 353 (4660)
17	C_6H_5	Se	268 sh (79 270), 349 (5810)
18	C_6H_4Me-*p*	Se	270 sh (66 210), 355 (5440)
19	C_6H_4F-*p*	Se	270 sh (55 610), 354 (5370)

there were no significant changes in the emission energies upon a change in the bis(diphenylphosphino)amine ligands. A similar red shift of the luminescence into the near-infrared (NIR) region at 77 K was observed in a related $Au_{10}Se_4$ core cluster.[7d]

Hexanuclear Gold(I) Complexes. Excitation of the hexanuclear complexes in the solid state and in solution with visible light at $\lambda \geq 400$ nm at room temperature and at 77 K results in intense emission in the orange-red region. The luminescence data of the hexanuclear complexes **12**, **13**, and **15**−**19** are summarized in Table 3, and the emission spectra of **12** and **16** in the solid state at 298 K are shown in Figure 4. The radiative lifetimes in the microsecond range are suggestive of a triplet parentage. With reference to the previous study of **14**,[7c] the emission is assigned to originate from triplet states of a ligand-to-metal charge-transfer character that mixed with metal-centered (ds/dp) states modified by Au···Au interactions (LMMCT; E→Au). This class of complexes has abnormally large Stokes shifts with values of > 1.5 eV between the lowest-energy excitation maximum and the emission maximum in solution at room temperature. This may suggest that the excited-state structure is highly distorted from that of the ground state. When compared with the orange emission observed in the room-temperature solid (λ_{em} = 592−700 nm), the red shift of the luminescence into the NIR region in dichloromethane solution (λ_{em} = 787 to >850 nm) can be ascribed to the larger structural changes that may occur in solution rather than in the rigid lattice of the solid.[7c,14] The low-energy emission of the selenido analogues is also red-shifted when compared to the sulfido counterparts (Table 3), which is consistent with the lower σ-donating capability of the sulfido than the selenido moiety. These, together with the lack of significant changes in the emission energies upon a change in the bis(dipenylphosphino)amine ligands, further substantiate the assignment of the emission as being from an LMMCT origin.

When the same types of bis(diphenylphosphino)aniline ligands are considered, it can be observed that the differences in the emission energies in the solid state and in solution that were due to the LMMCT origin, increase on going from the decanuclear gold(I) complexes to the hexanuclear complexes. Such phenomenon might give an indication of the degree of rigidity of the clusters, and it can be tentatively concluded that the hexanuclear complexes have a more flexible and open structure compared to that of the decanuclear complexes. The core of the decanuclear complexes is somewhat protected by the aromatic rings of the diphosphine ligands at the outer shell. In contrast, the heterocubane core in the hexanuclear complexes seems to have a more open structure that is less well protected and is thus more sensitive to surrounding changes such as interaction with solvents.

Photochemical Properties. It is well-known that the excited state of a complex is usually a better and stronger reducing agent as well as a better oxidizing agent than the corresponding ground state, given the higher electron-donating ability and the higher electron affinity due to the promotion of an electron from the highest occupied molecular orbital (HOMO) to the lowest unoccupied molecular orbital (LUMO), which generates an electron in a higher-lying orbital and a hole in a lower-energy orbital upon excitation. In view of the electron-richness of the polynuclear d^{10} metal complexes, a number of studies were undertaken to probe their excited-state reactivities. The complexes were shown to be photoredox active and could be readily quenched by a series of electron acceptors through bimolecular processes. Provided that the excited state exhibits long luminescence lifetimes, kinetics on the bimolecular quenching processes can be studied. In view of the related studies on the long-lived phosphorescent states of the tetranuclear copper(I) sulfido complexes,[3d,g] which were shown to possess rich photoredox behavior and undergo facile electron-transfer reactions with a series of electron acceptors, it is believed that similar study on the polynuclear gold(I) sulfido complexes would be interesting and informative.

Of the polynuclear gold(I) sulfido complexes studied, the decanuclear complex **3** was selected for photochemical reactivity studies because of its stability in solution and the presence of long-lived phosphorescent states, which might allow sufficient time for bimolecular reaction to occur. The nature of the bimolecular photochemical reactions between the complexes and pyridinium acceptors was believed to be electron-transfer rather than energy-transfer in nature since the triplet-state energy of the pyridinium ion was too high for any appreciable energy transfer reaction from the excited state of the complex to occur.

To establish the electron-transfer nature of the quenching reaction, nanosecond transient absorption spectroscopy was employed to provide direct spectroscopic evidence for the mechanism. Figure 5 reveals a transient absorption difference spectrum of the laser flash photolysis of a degassed acetone solution of **3** (4.8×10^{-5} M) and 4-methoxycarbonyl-*N*-methylpyridinium hexafluorophosphate (1.0×10^{-2} M) containing 0.1 M tetra-*n*-butylammonium hexafluorophosphate

Table 2. Luminescence Data for the Decanuclear Gold(I) Complexes $[Au_{10}\{\mu\text{-}Ph_2PN(R)PPh_2\}_4(\mu_3\text{-}E)_4]^{2+}$ (1−11)

complex	R	E	medium (*T*/K)	emission λ/nm ($\tau_o/\mu s$)[a]
1	^{n}Pr	S	solid (298)	522, 657 (0.23, 1.28)
			solid (77)	526, 662 (3.77)
			CH_2Cl_2 (298)	510, 759 (0.10)
2	C_6H_5	S	solid (298)	522 (0.9, 0.2), 715 (4.6, 0.7)
			solid (77)	527 (2.8, 0.3), 664 (5.2, 0.3)
			CH_2Cl_2 (298)	520, 794 (0.2)
3	C_6H_4Me-*p*	S	solid (298)	527 (1.0, 0.3), 700 (4.1, 0.7)
			solid (77)	529 (2.7, 0.4), 672 (8.0, 1.6)
			CH_2Cl_2 (298)	517, 794 (0.2)
4	C_6H_4OMe-*p*	S	solid (298)	528 (0.7, 0.1), 740 (6.2, 1.1)
			solid (77)	530 (3.0, 0.3), 665 (16.3, 3.0)
			CH_2Cl_2 (298)	517, 800 (0.2)
5	C_6H_4Cl-*p*	S	solid (298)	531 (0.7, 0.2), 704 (4.3, 0.7)
			solid (77)	528 (3.1, 0.6), 693 (6.9, 0.9)
			CH_2Cl_2 (298)	519, 796 (0.2)
6	C_6H_4Br-*p*	S	solid (298)	529 (0.7, 0.1), 713 (5.2, 0.9)
			solid (77)	532 (3.2, 0.9), 672 (8.2, 2.1)
			CH_2Cl_2 (298)	531, 798 (0.2)
7	C_6H_4F-*p*	S	solid (298)	534 (0.9, 0.2)
			solid (77)	533 (3.4, 0.5), 658 (18.0, 4.7)
			CH_2Cl_2 (298)	519, 798 (0.2)
8	^{n}Pr	Se	solid (298)	584 (0.3)
			solid (77)	567 (4.3), 703 (2.9)
			CH_2Cl_2 (298)	554 (<0.1)
9	C_6H_5	Se	solid (298)	574 (0.1)
			solid (77)	663 (31.6)
			CH_2Cl_2 (298)	590 (4.4), 704 (1.4)
10	C_6H_4Me-*p*	Se	solid (298)	577 (1.3)
			solid (77)	595 (2.7), 703 (0.6)
			CH_2Cl_2 (298)	568 (<0.1)
11	C_6H_4F-*p*	Se	solid (298)	597 (1.0)
			solid (77)	592 (4.2), 725 (0.8)
			CH_2Cl_2 (298)	568 (<0.1)

[a] The determination of the respective luminescence quantum yields was hindered by the absence of appropriate reference compound with similar absorption and luminescence properties, i.e., having similarly unusual large Stokes shifts. The dual luminescence nature further complicated the determination with the requirement of obtaining a complete full-spread spectrum covering all the way from the visible to the near-infrared region.

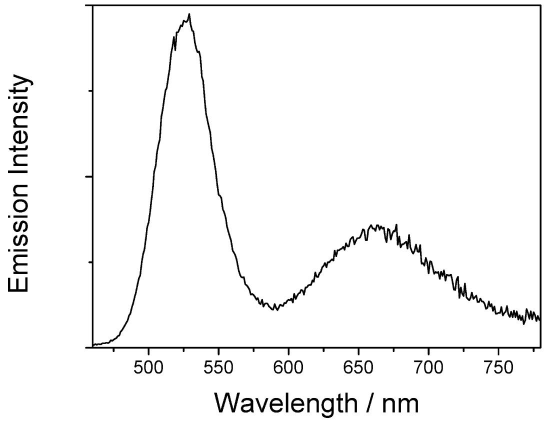

Figure 3. Solid-state emission spectrum of **2** at 77 K.

as the supporting electrolyte. It is dominated by a band at ca. 400 nm, which is characteristic of the pyridinyl radical and matched well with the literature-reported spectrum of the reduced radical of 4-methoxycarbonyl-*N*-methylpyridinium ion.[15] The reaction mechanism is shown below:

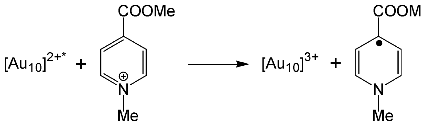

■ CONCLUSIONS

A family of high-nuclearity gold(I) chalcogenides, namely, sulfido and selenido complexes containing different bridging bis(diphenylphosphino)amine ligands with nuclearities of ten ($[Au_{10}\{\mu\text{-}Ph_2PN(R)PPh_2\}_4(\mu_3\text{-}E)_4]^{2+}$) and six ($[Au_6\{\mu\text{-}Ph_2PN(R)PPh_2\}_3(\mu_3\text{-}E)_2]^{2+}$), has been successfully prepared. The complex cations of Au_{10} possess propeller-like structures, and those of Au_6 have distorted cubane structures with the presence of short intramolecular gold⋯gold distances, as revealed by X-ray structural analysis. The differences in nuclearities and chalcogenido ligands give rise to different emission properties. The complexes show intense green and/or orange phosphorescence, which have been tentatively assigned to originate from the excited states derived from the phosphine-centered intraligand transition and metal-centered (ds/dp) mixed with LMMCT (E→Au) transition, respectively, upon photoexcitation in the solid state and in solution at ambient and low

Table 3. Luminescence Data for the Hexanuclear Gold(I) Complexes $[Au_6\{\mu\text{-}Ph_2PN(R)PPh_2\}_3(\mu_3\text{-}E)_2]^{2+}$ (12–19)

complex	R	E	medium (T/K)	emission λ/nm (τ_o/μs)
12	^{n}Pr	S	solid (298)	594 (19.6, 2.9)
			solid (77)	592 (23.7, 2.0)
			CH_2Cl_2 (298)	787 (0.9)
13	C_6H_5	S	solid (298)	624 (25.0, 4.9)
			solid (77)	617 (30.3, 4.4)
			CH_2Cl_2 (298)	810 (4.0)
14	C_6H_4Me-*p*	S	solid (298)	635 (14.3, 2.5)
			solid (77)	603
			CH_2Cl_2 (298)	810 (3.6)
15	C_6H_4OMe-*p*	S	solid (298)	630 (12.4, 2.0)
			solid (77)	602 (21.4, 2.4)
			CH_2Cl_2 (298)	808 (3.5)
16	^{n}Pr	Se	solid (298)	697 (29.0)
			solid (77)	668 (42.8)
			CH_2Cl_2 (298)	---[a]
17	C_6H_5	Se	solid (298)	700 (24.6)
			solid (77)	663 (31.6)
			CH_2Cl_2 (298)	803 (0.3)
18	C_6H_4Me-*p*	Se	solid (298)	724 (10.1)
			solid (77)	691 (33.8)
			CH_2Cl_2 (298)	810 (<0.1)
19	C_6H_4F-*p*	Se	solid (298)	674 (22.1)
			solid (77)	645 (35.6)
			CH_2Cl_2 (298)	808 (0.4)

[a] Emission maximum >850 nm.

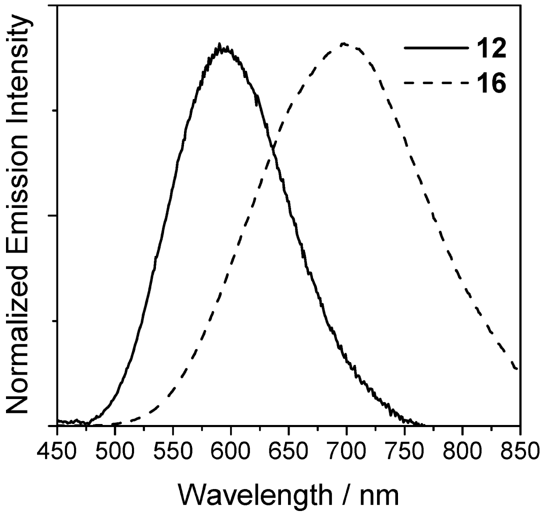

Figure 4. Solid-state emission spectra of **12** and **16** at 298 K.

temperature, and such phosphorescence was found to be relatively insensitive to the nature of the substituents on the bridging diphosphine ligands. In particular, the photoluminescence of the polynuclear gold(I) selenido complexes has been further extended into the NIR region, representing a new class of versatile NIR triplet emitters, which is the first of its kind. The photoredox properties of the high-nuclearity gold(I) chalcogenides have also been probed by transient absorption spectroscopy.

■ EXPERIMENTAL SECTION

Materials and Reagents. The ligands bis(diphenylphosphino)-*n*-propylamine, bis(diphenylphosphino)aniline, bis(diphenylphosphino)-4-methylaniline, bis(diphenylphosphino)-4-methoxylaniline, bis(diphenylphosphino)-4-fluoroaniline, bis(diphenylphosphino)-4-chloroaniline, and bis(diphenylphosphino)-4-bromoaniline were synthesized according to published procedures using the appropriate substituted anilines.[16] The binuclear gold(I) chloride precursors, $[Au_2\{\mu\text{-}Ph_2PN(R)PPh_2\}Cl_2]$, were synthesized according to literature procedures.[10b,17] Hydrogen sulfide was freshly generated by reaction of solid iron(II) sulfide with dilute hydrochloric acid, washed with deionized water in a bubbler, and dried by passing through a column of anhydrous calcium chloride before use. Pyridine (Acros, 99+%) was distilled over potassium hydroxide and stored in the presence of potassium hydroxide prior to use. Na_2Se was generated in situ via the reaction of Se powder (Acros, 99.5%) with sodium borohydride (Acros, 98+%) in tetrahydrofuran solution under anhydrous and anaerobic conditions. Ammonium hexafluorophosphate (Strem, 99.5%) and lithium perchlorate trihydrate (Strem, 98%) were purchased and used as received. All solvents were purified and distilled in a nitrogen atmosphere using standard procedures prior to use. All other reagents were of analytical grade and were used as received.

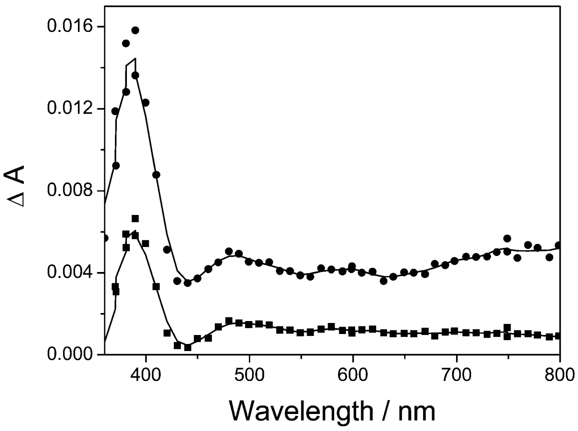

Figure 5. Transient absorption difference spectra recorded at 10 μs (●) and 40 μs (■) after the laser flash for a degassed acetone solution of compound **3** (4.8×10^{-5} M) and 4-methoxycarbonyl-*N*-methylpyridinium hexafluorophosphate (1.0×10^{-2} M) in the presence of ${}^{n}Bu_4NPF_6$ (0.10 M).

The pyridinium salts for quenching studies were prepared by refluxing the corresponding pyridine and alkylating agent in an acetone–ethanol (1:1 v/v) solution for 4 h, followed by metathesis reaction using ammonium hexafluorophosphate in water and subsequent recrystallization from acetonitrile–diethyl ether. The gold(I) sulfido complexes were synthesized according to the previous procedures for **1**[7b] and **14**[7c] with modification.

Synthesis. *$[Au_{10}(\mu\text{-}Ph_2PN({}^{n}Pr)PPh_2)_4(\mu_3\text{-}S)_4](PF_6)_2$ (**1**) and $[Au_6\{\mu\text{-}Ph_2PN({}^{n}Pr)PPh_2\}_3(\mu_3\text{-}S)_2](PF_6)_2$ (**12**).* To a suspension of $[Au_2\{\mu\text{-}Ph_2PN({}^{n}Pr)PPh_2\}Cl_2]$ (200 mg, 0.22 mmol) in ethanol (8 mL) was added pyridine (2.5 mL). The reaction mixture was stirred at room temperature for one minute, and H_2S was bubbled into the solution mixture for 20 min. At the same time, the reaction mixture was allowed to warm to ca. 50 °C. The white suspension dissolved instantly, and a clear yellow solution was obtained. Removal of the solvents under vacuum yielded the greenish-yellow solid, which was washed with diethyl ether (2 × 5 mL) and redissolved in methanol (1 mL). Metathesis reaction with saturated ammonium hexafluorophosphate solution in methanol gave a greenish-yellow solid. Subsequent recrystallization by the diffusion of diethyl ether vapor into an acetone solution yielded **1** as greenish-yellow crystals (132 mg, 72%) and **12** as white powder (38 mg, 18%).

1: ${}^{1}H$ NMR (300 MHz, CD_2Cl_2, 298 K, Me_4Si): δ 0.04 (m, 12 H, $-CH_3$), 0.27 (m, 4 H, $-CH_2-$), 0.85 (m, 4 H, $-CH_2-$), 2.33 (m, 4 H, $-NCH_2-$), 2.80 (m, 4 H, $-NCH_2-$), 6.83 (m, 8H, phenyl H), 7.12–7.83 (m, 72 H, phenyl H); ${}^{31}P\{{}^{1}H\}$ NMR (202 MHz, CD_2Cl_2, 298 K): δ 83.1, 85.5 (dd, J_{P-P} = 115 Hz); MS (positive-ion fast atom bombardment (FAB)): *m*/*z*: 1903 $[M{-}2PF_6]^{2+}$; MS (positive-ESI): *m*/*z*: 1903 $[M{-}2PF_6]^{2+}$; MS (negative-ESI): *m*/*z*: 145 $[PF_6]^-$; elemental analysis calcd (%) for $C_{108}H_{108}Au_{10}N_4F_{12}P_{10}S_4{\cdot}(CH_3)_2CO$: C 32.08, H 2.76, N 1.38; found: C 32.34, H 2.75, N 1.43; molar conductivity: $\Lambda_M = 262\ \Omega^{-1}\ cm^2\ mol^{-1}$ (1:2 electrolyte). **12**: ^1H NMR (500 MHz, acetone-d_6, 298 K): δ 0.04 (t, 9 H, $-CH_3$), 0.30−0.75 (v. br. m, 6 H, $-CH_2-$), 2.35−2.75 (m, 6 H, $-NCH_2-$), 6.92−7.93 (v. br. m, 60 H, phenyl H); VT ^1H NMR (500 MHz, CD_2Cl_2): 330 K: δ 0.04 (t, 9 H, $-CH_3$), 0.59 (m, 6 H, $-CH_2-$), 2.56 (m, 6 H, $-NCH_2-$), 6.90−8.00 (m, 60 H, phenyl H); 298 K: δ 0.04 (t, 9 H, $-CH_3$), 0.43 (br. m, 3 H, $-CH_2-$), 0.70 (br. m, 3 H, $-CH_2-$), 2.49 (m, 3 H, $-NCH_2-$), 2.62 (m, 3 H, $-NCH_2-$), 6.90−8.00 (br. m, 60 H, phenyl H); 273 K: δ 0.03 (t, 9 H, $-CH_3$), 0.36 (m, 3 H, $-CH_2-$), 0.73 (m, 3 H, $-CH_2-$), 2.37 (m, 3 H, $-NCH_2-$), 2.68 (m, 3 H, $-NCH_2-$), 7.06 (m, 12 H, phenyl H), 7.37−7.46 (m, 18 H, phenyl H), 7.68 (m, 24 H, phenyl H), 7.83 (m, 6 H, phenyl H); $^{31}P\{^1H\}$ NMR (202 MHz, acetone-d_6, 298 K): δ 79.3; MS (positive-ion FAB): *m*/*z*: 2672 $[M{-}PF_6]^+$, 1263 $[M{-}2PF_6]^{2+}$; MS (positive-ESI): *m*/*z*: 1264 $[M{-}2PF_6]^{2+}$; elemental analysis calcd (%) for $C_{81}H_{81}Au_6N_3F_{12}P_8S_2$: C 34.52, H 2.90, N 1.49; found: C 34.36, H 2.84, N 1.43.

*$[Au_{10}\{\mu\text{-}Ph_2PN(C_6H_5)PPh_2\}_4(\mu_3\text{-}S)_4](ClO_4)_2$ (**2**) and $[Au_6\{\mu\text{-}Ph_2PN(C_6H_5)PPh_2\}_3(\mu_3\text{-}S)_2](ClO_4)_2$ (**13**).* **2** and **13** were synthesized according to a procedure similar to that of **1** and **12**, respectively, except $[Au_2\{\mu\text{-}Ph_2PN(C_6H_5)PPh_2\}Cl_2]$ (200 mg, 0.22 mmol) was used in place of $[Au_2\{\mu\text{-}Ph_2PN(^nPr)PPh_2\}Cl_2]$. $LiClO_4{\cdot}3H_2O$ was used in the metathesis reaction instead of NH_4PF_6 to give the corresponding ClO_4^- salts. First crystallization by the diffusion of diethyl ether vapor into an acetone solution and subsequent recrystallization by the diffusion of diethyl ether vapor into a dichloromethane solution yielded **2** as greenish-yellow crystals (72 mg, 40%) and **13** as colorless crystals (76 mg, 37%). **2**: ^1H NMR (500 MHz, CD_2Cl_2, 298 K, Me_4Si): δ 6.11 (d, 4 H, *J* = 7.6 Hz, aromatic H), 6.38 (d, 4 H, *J* = 7.6 Hz, aromatic H), 6.66 (t, 4 H, *J* = 7.6 Hz, aromatic H), 6.73 (t, 4 H, *J* = 7.6 Hz, aromatic H), 6.87−6.92 (m, 12 H, aromatic H + $-PPh_2$), 7.14−7.17 (m, 8 H, $-PPh_2$), 7.24−7.63 (m, 60 H, $-PPh_2$), 7.78 (m, 4H, $-PPh_2$); $^{31}P\{^1H\}$ NMR (202 MHz, CD_2Cl_2, 298 K): δ 87.2, 89.2 (dd, J_{P-P} = 109 Hz); MS (positive-ion FAB): *m*/*z*: 4040 $[M{-}ClO_4]^+$, 1972 $[M{-}2ClO_4]^{2+}$; MS (positive-ESI): *m*/*z*: 1971 $[M{-}2ClO_4]^{2+}$; MS (negative-ESI): *m*/*z*: 145 $[PF_6]^-$; elemental analysis calcd (%) for $C_{120}H_{100}Au_{10}Cl_2N_4O_8P_8S_4{\cdot}2CH_2Cl_2$: C 33.98, H 2.43, N 1.30; found: C 33.98, H 2.24, N 1.23; **13**: ^1H NMR (500 MHz, acetone-d_6, 298 K): δ = 6.30 (d, 6 H, *J* = 7.9 Hz, aromatic H), 6.80 (dd, 6 H, *J* = 7.4 Hz, 7.9 Hz, aromatic H), 7.00 (t, 3 H, *J* = 7.4 Hz, aromatic H), 7.28−7.32 (m, 24 H, $-PPh_2$), 7.43−7.48 (m, 18 H, $-PPh_2$), 7.65−7.68 (m, 6 H, $-PPh_2$), 7.73−7.75 (m, 12 H, $-PPh_2$); $^{31}P\{^1H\}$ NMR (202 MHz, acetone-d_6, 298 K): δ 82.8; MS (positive-ion FAB): *m*/*z*: 1315 $[M{-}2ClO_4]^{2+}$; MS (positive-ESI): *m*/*z*: 1315 $[M{-}2ClO_4]^{2+}$; elemental analysis calcd (%) for $C_{90}H_{75}Au_6Cl_2N_3O_8P_6S_2{\cdot}CH_2Cl_2$: C 37.51, H 2.66, N 1.44; found: C 37.40, H 2.58, N 1.47.

*$[Au_{10}\{\mu\text{-}Ph_2PN(C_6H_4CH_3\text{-}p)PPh_2\}_4(\mu_3\text{-}S)_4](ClO_4)_2$ (**3**) and $[Au_6\{\mu\text{-}Ph_2PN(C_6H_4CH_3\text{-}p)PPh_2\}_3(\mu_3\text{-}S)_2](ClO_4)_2$ (**14**).* **3** and **14** were synthesized according to a procedure similar to that of **2** and **13**, respectively, except $[Au_2\{\mu\text{-}Ph_2PN(C_6H_4CH_3\text{-}p)PPh_2\}Cl_2]$ (200 mg, 0.21 mmol) was used in place of $[Au_2\{\mu\text{-}Ph_2PN(C_6H_5)PPh_2\}Cl_2]$. **3** was isolated as greenish-yellow crystals (70 mg, 39%), and **14** was isolated as colorless crystals (102 mg, 50%). **3**: ^1H NMR (500 MHz, CD_2Cl_2, 298 K, Me_4Si): δ 2.03 (s, 12 H, $-CH_3$), 5.97 (d, 4 H, *J* = 8.4 Hz, aromatic H) 6.23 (d, 4 H, *J* = 8.0 Hz, aromatic H), 6.45 (d, 4 H, *J* = 8.4 Hz, aromatic H), 6.52 (d, 4 H, *J* = 8.0 Hz, aromatic H), 6.88−6.91 (m, 8 H, $-PPh_2$), 7.13−7.17 (m, 8 H, $-PPh_2$), 7.26−7.61 (m, 60 H, $-PPh_2$), 7.74−7.77 (m, 4H, $-PPh_2$); $^{31}P\{^1H\}$ NMR (202 MHz, CD_2Cl_2, 298 K): δ 87.3, 88.7 (dd, J_{P-P} = 111 Hz); MS (positive-ion FAB): *m*/*z*: 1999 $[M{-}2ClO_4]^{2+}$; MS (positive-ESI): *m*/*z*: 1999 $[M{-}2ClO_4]^{2+}$; MS (negative-ESI): *m*/*z*: 99 $[ClO_4]^-$; elemental analysis calcd (%) for $C_{124}H_{108}Au_{10}Cl_2N_4O_8P_8S_4{\cdot}(3/2)CH_2Cl_2$: C 34.84, H 2.59, N 1.30; found: C 34.84, H 2.42, N 1.27; **14**: ^1H NMR (500 MHz, acetone-d_6, 298 K): δ 2.02 (s, 9 H, $-CH_3$), 6.16 (d, 6 H, *J* = 8.3 Hz, aromatic H), 6.61 (d, 6 H, *J* = 8.3 Hz, aromatic H), 7.28−7.31 (m, 24 H, $-PPh_2$), 7.43−7.46 (m, 18 H, $-PPh_2$), 7.65−7.74 (m, 18 H, $-PPh_2$); $^{31}P\{^1H\}$ NMR (202 MHz, acetone-d_6, 298 K): δ 82.7; MS (positive-ion FAB): *m*/*z*: 2772 $[M{-}ClO_4]^+$, 1336 $[M{-}2ClO_4]^{2+}$; MS (positive-ESI): *m*/*z*: 2772 $[M{-}ClO_4]^+$, 1336 $[M{-}2ClO_4]^{2+}$; MS (negative-ESI): *m*/*z*: 99 $[ClO_4]^-$; elemental analysis calcd (%) for $C_{93}H_{81}Au_6Cl_2N_3O_8P_6S_2{\cdot}2CH_2Cl_2$: C 37.52, H 2.82, N 1.38; found: C 37.49, H 2.52, N 1.34.

*$[Au_{10}\{\mu\text{-}Ph_2PN(C_6H_4OCH_3\text{-}p)PPh_2\}_4(\mu_3\text{-}S)_4](ClO_4)_2$ (**4**) and $[Au_6\{\mu\text{-}Ph_2PN(C_6H_4OCH_3\text{-}p)PPh_2\}_3(\mu_3\text{-}S)_2](ClO_4)_2$ (**15**).* **4** and **15** were synthesized according to a procedure similar to that of **2** and **13**, respectively, except $[Au_2\{\mu\text{-}Ph_2PN(C_6H_4OCH_3\text{-}p)PPh_2\}Cl_2]$ (200 mg, 0.21 mmol) was used in place of $[Au_2\{\mu\text{-}Ph_2PN(C_6H_5)PPh_2\}Cl_2]$. **4** was isolated as yellow needles (50 mg, 28%), and **15** was isolated as colorless crystals (57 mg, 30%). **4**: ^1H NMR (500 MHz, CD_2Cl_2, 298 K, Me_4Si): δ 3.53 (s, 12 H, $-OCH_3$), 6.00 (m, 4 H, aromatic H), 6.14−6.16 (m, 4 H, aromatic H), 6.20−6.27 (m, 8 H, aromatic H), 6.88−6.92 (m, 8 H, $-PPh_2$), 7.16−7.20 (m, 8 H, $-PPh_2$), 7.27−7.30 (m, 4 H, $-PPh_2$), 7.34−7.53 (m, 48 H, $-PPh_2$), 7.57−7.61 (m, 8 H, $-PPh_2$), 7.74−7.77 (m, 4H, $-PPh_2$); $^{31}P\{^1H\}$ NMR (202 MHz, CD_2Cl_2, 298 K): δ 87.9, 89.2 (dd, J_{P-P} = 113 Hz); MS (positive-ion FAB): *m*/*z*: 2031 $[M{-}2ClO_4]^{2+}$; elemental analysis calcd (%) for $C_{124}H_{108}Au_{10}Cl_2N_4O_{12}P_8S_4{\cdot}2CH_2Cl_2$: C 34.14, H 2.55, N 1.26; found: C 34.01, H 2.42, N 1.18; **15**: ^1H NMR (500 MHz, acetone-d_6, 298 K): δ 3.53 (s, 9 H, $-OCH_3$), 6.17−6.19 (m, 6 H, aromatic H), 6.30−6.33 (m, 6 H, aromatic H), 7.29−7.48 (m, 24 H, $-PPh_2$), 7.66−7.69 (m, 18 H, $-PPh_2$), 7.71−7.72 (m, 18 H, $-PPh_2$); $^{31}P\{^1H\}$ NMR (202 MHz, acetone-d_6, 298 K): δ 83.2; MS (positive-ion FAB): 1360 $[M{-}2ClO_4]^{2+}$; MS (positive-ESI): *m*/*z*: 1360 $[M{-}2ClO_4]^{2+}$; elemental analysis calcd (%) for $C_{93}H_{81}Au_6Cl_2N_3O_{11}P_6S_2{\cdot}(3/2)CH_2Cl_2$: C 37.58, H 2.53, N 1.45; found: C 37.63, H 2.48, N 1.45.

*$[Au_{10}\{\mu\text{-}Ph_2PN(C_6H_4Cl\text{-}p)PPh_2\}_4(\mu_3\text{-}S)_4](ClO_4)_2$ (**5**).* The titled complex was synthesized according to a procedure similar to that of **2**, except $[Au_2\{\mu\text{-}Ph_2PN(C_6H_4Cl\text{-}p)PPh_2\}Cl_2]$ (200 mg, 0.21 mmol) was used in place of $[Au_2\{\mu\text{-}Ph_2PN(C_6H_5)PPh_2\}Cl_2]$. **5** was isolated as yellow needles (60 mg, 34%). **5**: ^1H NMR (500 MHz, CD_2Cl_2, 298 K): δ 6.02−6.04 (m, 4 H, aromatic H), 6.31−6.33 (m, 4 H, aromatic H), 6.63−6.66 (m, 4 H, aromatic H), 6.71−6.73 (m, 4 H, aromatic H), 6.89−6.93 (m, 8 H, $-PPh_2$), 7.20−7.24 (m, 8 H, $-PPh_2$), 7.29−7.32 (m, 4 H, $-PPh_2$), 7.35−7.59 (m, 48 H, $-PPh_2$), 7.60−7.64 (m, 8 H, $-PPh_2$), 7.78−7.82 (m, 4H, $-PPh_2$); $^{31}P\{^1H\}$ NMR (202 MHz, CD_2Cl_2, 298 K): δ 87.9, 89.4 (dd, J_{P-P} = 108 Hz); MS (positive-ion FAB): *m*/*z* 2040 $[M{-}2ClO_4]^{2+}$; MS(positive ESI): *m*/*z* 2040 $[M{-}2ClO_4]^{2+}$; MS(negative ESI): *m*/*z* 99 $[ClO_4]^-$; elemental analysis calcd (%) for $[Au_{10}\{Ph_2PN(C_6H_4Cl\text{-}p)PPh_2\}_4S_4](ClO_4)_2{\cdot}3CH_2Cl_2$: C 32.57, H 2.27, N 1.24; found: C 32.53, H 2.13, N 1.17.

*$[Au_{10}\{\mu\text{-}Ph_2PN(C_6H_4Br\text{-}p)PPh_2\}_4(\mu_3\text{-}S)_4](ClO_4)_2$ (**6**).* The titled complex was synthesized according to a procedure similar to that of **2**, except $[Au_2\{\mu\text{-}Ph_2PN(C_6H_4Br\text{-}p)PPh_2\}Cl_2]$ (200 mg, 0.20 mmol) was used in place of $[Au_2\{\mu\text{-}Ph_2PN(C_6H_5)PPh_2\}Cl_2]$. **6** was isolated as yellow needles (35 mg, 20%). **6**: ^1H NMR (500 MHz, CD_2Cl_2, 298 K): δ 5.95−5.97 (m, 4 H, aromatic H), 6.24−6.26 (m, 4 H, aromatic H), 6.79−6.81 (m, 4 H, aromatic H), 6.71−6.73 (m, 4 H, aromatic H), 6.89−6.93 (m, 8 H, $-PPh_2$), 6.86−6.92 (m, 12 H, aromatic H and $-PPh_2$), 7.20−7.23 (m, 8 H, $-PPh_2$), 7.29−7.32 (m, 4 H, $-PPh_2$), 7.33−7.58 (m, 48 H, $-PPh_2$), 7.60−7.64 (m, 8 H, $-PPh_2$), 7.78−7.81 (m, 4H, $-PPh_2$); $^{31}P\{^1H\}$ NMR (202 MHz, CD_2Cl_2, 298 K): δ 87.4, 89.4 (dd, J_{P-P} = 108 Hz); MS (positive-ion FAB): *m*/*z* 2129 $[M{-}2ClO_4]^{2+}$; elemental analysis calcd (%) for $C_{120}H_{96}Au_{10}F_4Br_2N_4O_8P_8S_4{\cdot}3CH_2Cl_2$: C 31.34, H 2.18, N 1.19; found: C 31.39, H 2.11, N 0.75.

*$[Au_{10}\{\mu\text{-}Ph_2PN(C_6H_4F\text{-}p)PPh_2\}_4(\mu_3\text{-}S)_4](ClO_4)_2$ (**7**).* The titled complex was synthesized according to a procedure similar to that of **2**, except $[Au_2\{\mu\text{-}Ph_2PN(C_6H_4F\text{-}p)PPh_2\}Cl_2]$ (200 mg, 0.21 mmol) was used in place of $[Au_2\{\mu\text{-}Ph_2PN(C_6H_5)PPh_2\}Cl_2]$. **7** was isolated as yellow needles (110 mg, 62%). **7**: ^1H NMR (500 MHz, CD_2Cl_2, 298 K): δ 6.06−6.08 (m, 4 H, aromatic H), 6.35−6.39 (m, 8 H, aromatic H), 6.42−6.46 (m, 4 H, aromatic H), 6.89−6.93 (m, 8 H, $-PPh_2$), 7.19−7.23 (m, 8 H, $-PPh_2$), 7.29−7.31 (m, 4 H, $-PPh_2$), 7.37−7.59 (m, 48 H, $-PPh_2$), 7.60−7.64 (m, 8 H, $-PPh_2$), 7.78−7.81 (m, 4H, $-PPh_2$); $^{31}P\{^1H\}$ NMR (202 MHz, CD_2Cl_2, 298 K): δ 88.1, 89.5 (dd, J_{P-P} = 108 Hz); MS (positive-ion FAB): *m*/*z* 2007 $[M{-}2ClO_4]^{2+}$;

elemental analysis calcd (%) for $C_{120}H_{96}Au_{10}F_4Cl_2N_4O_8P_8S_4 \cdot 3CH_2Cl_2$: C 33.05, H 2.30, N 1.25; found: C 32.97, H 2.23, N 1.11.

$[Au_{10}\{\mu\text{-}Ph_2PN(^nPr)PPh_2\}_4(\mu_3\text{-}Se)_4](ClO_4)_2$ **(8)** *and* *$[Au_6\{\mu\text{-}Ph_2PN(^nPr)PPh_2\}_3(\mu_3\text{-}Se)_2](PF_6)_2$* **(16)**. To a stirred solution of $[Au_2\{\mu\text{-}Ph_2PN(^nPr)PPh_2\}Cl_2]$ (200 mg, 0.22 mmol) in dichloromethane (20 mL) was added an excess of Na_2Se in a dropwise manner under anhydrous and anaerobic conditions. The reaction mixture immediately turned yellow, and it was allowed to stir for 2 d at room temperature. The reaction mixture was filtered and evaporated to dryness under reduced pressure, and the residue was redissolved in methanol and filtered. Metathesis reaction with a saturated solution of $LiClO_4 \cdot 3H_2O$ in methanol gave the product as a yellow powder, which was washed with diethyl ether. Subsequent recrystallization by the diffusion of diethyl ether vapor into a dichloromethane solution of the product yielded **8** as yellow crystals (85 mg, 46%). A white powder was obtained from the evaporation of the diethyl ether washings of the metathesized products. NH_4PF_6 was used in the metathesis reaction of complex **16** instead of $LiClO_4 \cdot 3H_2O$ to give the corresponding PF_6^- salt. Subsequent recrystallization of this white powder by layering *n*-hexane onto a concentrated dichloromethane solution of the complex gave **16** as colorless crystals (108 mg, 51%). **8**: ^1H NMR (300 MHz, acetone-d_6, 298 K): δ 0.07 (t, 12 H, $-CH_3$), 0.35−0.96 (v. br. m, 8 H, $-CH_2-$), 2.42−2.99 (v. br. m, 8 H, $-NCH_2-$), 6.92−7.78 (m, 80 H, $-PPh_2$); $^{31}P\{^1H\}$ NMR (202 MHz, acetone-d_6, 298 K): δ 81.11, 82.49 (dd, J_{P-P} = 111.7 Hz); MS (positive-ion FAB): *m*/*z* 1998 $[M-2ClO_4]^{2+}$; elemental analysis calcd (%) for $C_{108}H_{108}Au_{10}Cl_2N_4O_8P_8Se_4 \cdot 2(H_2O)$: C 30.67, H 2.67, N 1.32; found: C 30.37, H 2.66, N 1.45. **16**: ^1H NMR (300 MHz, acetone-d_6, 298 K): δ 0.05 (t, 9 H, $-CH_3$), 0.38−0.94 (v. br. m, 6 H, $-CH_2-$), 2.41−2.98 (v. br. m, 6 H, $-NCH_2-$), 7.09−7.97 (m, 60 H, $-PPh_2$); $^{31}P\{^1H\}$ NMR (202 MHz, acetone-d_6, 298 K): δ 79.98; MS (positive-ion FAB): *m*/*z* 1311 $[M-2PF_6]^{2+}$; elemental analysis calcd (%) for $C_{81}H_{81}Au_6F_{12}N_3P_8Se_2 \cdot (C_2H_5)_2O$: C 34.19, H 3.07, N 1.40; found: C 34.42, H 2.87, N 1.56.

$[Au_{10}\{\mu\text{-}Ph_2PN(C_6H_5)PPh_2\}_4(\mu_3\text{-}Se)_4](ClO_4)_2$ **(9)** *and* *$[Au_6\{\mu\text{-}Ph_2PN(C_6H_5)PPh_2\}_3(\mu_3\text{-}Se)_2](ClO_4)_2$* **(17)**. The titled complexes were synthesized according to the procedure similar to **8** and **16**, respectively, except $[Au_2\{\mu\text{-}Ph_2PN(C_6H_5)PPh_2\}Cl_2]$ (200 mg, 0.22 mmol) was used in place of $[Au_2\{\mu\text{-}Ph_2PN(^nPr)PPh_2\}Cl_2]$. Subsequent diffusion of diethyl ether vapor into a concentrated solution of the product resulted in the formation of yellow crystals of **9** (38 mg, 20%). $LiClO_4 \cdot 3H_2O$ was used in the metathesis reaction of complex **17** instead of NH_4PF_6 to give the corresponding ClO_4^- salt. Layering *n*-hexane onto a concentrated dichloromethane solution of the complex gave colorless crystals of **17** (52 mg, 24%). **9**: ^1H NMR (300 MHz, acetone-d_6, 298 K): δ 6.20 (d, 4 H, J_{H-H} = 7.8 Hz, aromatic H), 6.47 (d, 4H, J_{H-H} = 7.8 Hz, aromatic H), 6.55 (t, 4 H, J_{H-H} = 7.8 Hz, aromatic H), 6.98 (t, 4 H, J_{H-H} = 7.8 Hz, aromatic H), 7.36−7.43 (m, 12 H, aromatic H and $-PPh_2$), 7.49−7.59 (m, 8 H, $-PPh_2$), 7.67−7.70 (m, 60 H, $-PPh_2$), 7.71 (m, 4 H, $-PPh_2$); $^{31}P\{^1H\}$ NMR (202 MHz, acetone-d_6, 298 K): δ 85.17, 86.53 (dd, J_{P-P} = 110.0 Hz). MS (positive-ion FAB): *m*/*z* 2068 $[M-2ClO_4]^{2+}$; elemental analysis calcd (%) for $C_{120}H_{100}Au_{10}Cl_2N_4O_8P_8Se_4 \cdot C_6H_{14}$: C 34.27, H 2.60, N 1.27; found: C 34.33, H 2.55, N 1.02. **17**: ^1H NMR (300 MHz, acetone-d_6, 298 K): δ 6.35 (d, 6 H, J_{H-H} = 7.7 Hz, aromatic H), 6.78 (d, 6 H, J_{H-H} = 7.7 Hz, aromatic H), 6.98 (t, 3 H, J_{H-H} = 7.1 Hz, aromatic H), 7.29−7.76 (m, 60 H, $-PPh_2$); $^{31}P\{^1H\}$ NMR (202 MHz, acetone-d_6, 298 K): δ 77.71; MS (positive-ion FAB): *m*/*z* 1362 $[M-2ClO_4]^{2+}$; elemental analysis calcd (%) for $C_{90}H_{75}Au_6Cl_2N_3O_8P_6Se_2 \cdot 2CH_2Cl_2$: C 35.73, H 2.57, N 1.36; found: C 35.58, H 2.55, N 1.42.

$[Au_{10}\{\mu\text{-}Ph_2PN(C_6H_4CH_3\text{-}p)PPh_2\}_4(\mu_3\text{-}Se)_4](ClO_4)_2$ **(10)** *and* *$[Au_6\{\mu\text{-}Ph_2PN(C_6H_4CH_3\text{-}p)PPh_2\}_3(\mu_3\text{-}Se)_2](ClO_4)_2$* **(18)**. The titled complexes were synthesized according to the procedure similar to that for **9** and **17**, respectively, except $[Au_2\{\mu\text{-}Ph_2PN(C_6H_4CH_3\text{-}p)PPh_2\}Cl_2]$ (200 mg, 0.21 mmol) was used in place of $[Au_2\{\mu\text{-}Ph_2PN(^nPr)PPh_2\}Cl_2]$. Subsequent diffusion of diethyl ether vapor into a concentrated solution of the product resulted in the formation of yellow crystals of **10** (65 mg, 35%). Layering *n*-hexane onto a concentrated dichloromethane solution of the complex gave **18** as colorless crystals (78 mg, 38%). **10**: ^1H NMR (300 MHz, CD_2Cl_2, 298 K): δ 2.05 (s, 12 H, $-CH_3$), 6.16 (d, 4 H, J_{H-H} = 8.0 Hz, aromatic H), 6.35 (d, 4 H, J_{H-H} = 8.0 Hz, aromatic H), 6.51−6.62 (m, 8 H, $-PPh_2$), 7.02−7.13 (m, 16 H, $-PPh_2$), 7.29−7.73 (m, 60 H, $-PPh_2$), 7.79−7.86 (m, 4 H, $-PPh_2$); $^{31}P\{^1H\}$ NMR (202 MHz, acetone-d_6, 298 K): δ 85.03, 86.47 (J_{P-P}, 116.7 Hz); MS (positive-ion FAB): *m*/*z* 2096 $[M-2ClO_4]^{2+}$; elemental analysis calcd (%) for $Au_{10}Se_4C_{124}H_{108}N_4P_8Cl_2O_8 \cdot 2H_2O$: C 33.68; H 2.55; N 1.27; found: C 33.43, H 2.47; N 1.36. **18**: ^1H NMR (300 MHz, CD_2Cl_2, 298 K): δ 2.04 (s, 9 H, $-CH_3$), 6.35 (d, 6 H, J_{H-H} = 7.8 Hz, aromatic H), 6.79 (d, 6 H, J_{H-H} = 7.8 Hz, aromatic H), 7.29−7.78 (m, 60 H, $-PPh_2$); $^{31}P\{^1H\}$ NMR (202 MHz, acetone-d_6, 298 K): δ 77.78; MS (positive-ion FAB): *m*/*z* 1386 $[M-2ClO_4]^{2+}$; elemental analysis calcd (%) for $C_{93}H_{81}Au_6Cl_2N_3O_8Se_2P_6 \cdot H_2O$: C, 37.44; H, 2.80; N, 1.41. Found: C, 37.22; H, 2.82; N, 1.42.

$[Au_{10}\{\mu\text{-}Ph_2PN(C_6H_4F\text{-}p)PPh_2\}_4(\mu_3\text{-}Se)_4](ClO_4)_2$ **(11)** *and* *$[Au_6\{\mu\text{-}Ph_2PN(C_6H_4F\text{-}p)PPh_2\}_3(\mu_3\text{-}Se)_2](PF_6)_2$* **(19)**. The titled complexes were synthesized according to the procedure similar to that for **9** and **17**, respectively, except $[Au_2\{\mu\text{-}Ph_2PN(C_6H_4F\text{-}p)PPh_2\}Cl_2]$ (200 mg, 0.21 mmol) was used in place of $[Au_2\{\mu\text{-}Ph_2PN(^nPr)PPh_2\}Cl_2]$. NH_4PF_6 was used in the metathesis reaction of complex **19** instead of $LiClO_4 \cdot 3H_2O$ to give the corresponding PF_6^- salt. Subsequent recrystallization by the diffusion of diethyl ether vapor into an acetone solution gave yellow crystals of **11** (48 mg, 26%). The crystalline form of complex **19** (66 mg, 30%) was obtained by layering *n*-hexane onto a concentrated dichloromethane solution of the complex. **11**: ^1H NMR (300 MHz, acetone-d_6, 298 K): δ 6.53−6.58 (m, 8 H, aromatic H), 7.01−7.02 (m, 8 H, aromatic H), 7.40−7.74 (m, 80 H, $-PPh_2$); $^{31}P\{^1H\}$ NMR (202 MHz, acetone-d_6, 298 K): δ 85.55, 87.08 (dd, J_{P-P} = 114.0 Hz); MS (positive-ion FAB): *m*/*z* 2102 $[M-2ClO_4]^{2+}$; elemental analysis calcd (%) for $C_{120}H_{96}Au_{10}Cl_2F_4N_4O_8P_8Se_4$: C 32.74, H 2.20, N 1.27; found: C 32.50, H 2.25, N 1.19. **19**: ^1H NMR (300 MHz, acetone-d_6, 298 K): δ 6.39−6.40 (m, 6 H, aromatic H), 6.55−6.59 (m, 6 H, aromatic H), 7.31−7.77 (m, 60 H, $-PPh_2$); $^{31}P\{^1H\}$ NMR (202 MHz, acetone-d_6, 298 K): δ 78.27; MS (positive-ion FAB): *m*/*z* 1390 $[M-2PF_6]^{2+}$; elemental analysis calcd (%) for $C_{90}H_{72}Au_6F_{15}N_3P_8Se_2$: C 35.23, H 2.37, N 1.37; found: C 35.25, H 2.41, N 1.52.

Physical Measurements and Instrumentation. ^1H NMR spectra were recorded on a Bruker DRX-500 (500 MHz), Bruker DPX-300 (300 MHz), or JEOL JNM-GSX270 (270 MHz) multinuclear Fourier transform (FT) NMR spectrometer with chemical shifts (δ, ppm) reported relative to tetramethylsilane, $SiMe_4$. ^{31}P NMR spectra were recorded on a Bruker DRX-500 (202 MHz) FT-NMR spectrometer with chemical shifts reported relative to 85% H_3PO_4. Elemental analyses of all the newly synthesized metal complexes were performed either at the Butterworth Laboratories Ltd. or on a Carlo Erba 1106 elemental analyzer at the Institute of Chemistry, the Chinese Academy of Sciences in Beijing. All positive-ion FAB mass spectra were recorded on a Finnigan MAT95 mass spectrometer. The electrospray ionization (ESI) mass spectra were recorded either on a Finnigan LCQ mass spectrometer at The University of Hong Kong or on a Perkin-Elmer Sciex API365 quadrupole mass spectrometer at the City University of Hong Kong. All electronic absorption spectra were recorded on a Hewlett-Packard 8452A diode array spectrophotometer. Steady-state emission and excitation spectra recorded at room temperature and at 77 K were obtained on a Spex Fluorolog-2 Model F111 fluorescence spectrophotometer with or without corning filters. All solutions for photophysical studies were prepared in a two-compartment cell consisting of a 10 cm^3 Pyrex bulb equipped with a side arm to a 1 cm path length quartz cuvette and sealed from the atmosphere by a Rotaflo HP6/6 quick-release Teflon stopper. Solutions were degassed under high vacuum (limiting pressure $<10^{-3}$ Torr) with no less than four successive freeze−pump−thaw cycles. Solid-state photophysical measurements were carried out with solid samples loaded in a quartz tube inside a quartz-walled Dewar flask. Liquid nitrogen was placed into the Dewar flask for low-temperature (77 K) solid-state and glass photophysical measurements. Emission lifetime measurements were performed using a conventional laser system. The excitation source was the 355 nm output (third harmonic) of a Spectra-Physics Quanta-Ray Q-switched GCR-150−10 pulsed Nd:YAG laser. Luminescence decay signals were recorded on a Tektronix model TDS620A digital oscilloscope and analyzed using a program for exponential fits. Timeresolved transient absorption spectra were collected using the 355 nm output (third harmonic) of the Spectra-Physics Quanta-Ray Q-switched GCR-150−10 pulsed Nd:YAG laser as the excitation source, with the monitoring light beam generated from a 250 W quartz-tungsten-halogen lamp placed perpendicular to the excitation beam. The output of the quartz-tungsten-halogen lamp was wavelength-selected by passing through two monochromators (Oriel 77250, 1/8 m and 77200, 1/4 m). The transient absorption signals were detected by a Hamamatsu R928 photomultiplier tube, and the signal was amplified using a Tektronix AM 502 differential amplifier and digitized on a Tektronix Model TDS-620A (500 MHz, 2GS/s) digital oscilloscope interfaced to a personal computer for data acquisition and analysis.

Crystal Structure Determination. Single crystals of **3** suitable for X-ray diffraction studies were obtained from the slow diffusion of diethyl ether vapor into the concentrated acetonitrile solution of the complex. For **5**, single crystals suitable for X-ray diffraction studies were obtained from the slow diffusion of diethyl ether vapor into the concentrated acetone/dichloromethane (ca. 20:1 v/v) solution of the complex. Single crystals of **8**, **16**, and **17** suitable for X-ray diffraction studies were obtained from the layering of *n*-hexane onto a dichloromethane solution of the corresponding complexes. The X-ray diffraction data were collected at 28 °C on a Mar diffractometer with a 300 mm image plate detector using graphite monochromatized Mo−Kα radiation (λ = 0.71073 Å). The images were interpreted, and intensities were integrated using the program *DENZO*.[18] The structure was solved by direct methods employing the *SHELXS-97* program.[19] The Au, P, and S or Se atoms were located according to the direct methods. The positions of the other non-hydrogen atoms were found after successful refinement by full-matrix least-squares using the program *SHELXL-97*.[19] Full-matrix least-squares refinement on F^2 was used in the structure refinement. In addition to the molecular cation and counter-anions, dichloromethane solvent molecules were also located in the structures of complexes **5**, **8**, **16**, and **17**. Restraints have been applied in the structural refinement of these complexes. For complex **5**, because of the strong absorption of the gold atoms, no solvent molecules could be reliably located. The position of the perchlorate anion could not be located reliably because of the disorder of the O atoms, and the occupation of the anion has to be set to one-half manually. The O atoms of the perchlorate were restrained to have the same distances between each pair of them and the same thermal displacement parameter. For complex **8**, five dichloromethane solvent molecules were located. Two of them were well-located, while restraints were applied to the other three, assuming similar C−Cl bond lengths. One dichloromethane molecule was disordered into two positions by sharing one C−Cl bond. For this dichloromethane molecule, extra constraints were applied to assume the same thermal parameters for the copositioned C and Cl atoms and similar Cl···Cl distances. Similarly, restraints were applied to the two disordered dichloromethane molecules in complex **16**, assuming similar C−Cl bond lengths and Cl···Cl distances. For complex **17**, two perchlorate anions and two dichloromethane solvent molecules were located, in which one perchlorate anion was disordered. Restraints were applied to the disordered perchlorate, assuming similar Cl−O bond lengths and O···O bond distances. For all of the complexes, the positions of H atoms were calculated based on the riding mode with thermal parameters equal to 1.2 times those of the associated C atoms and participated in the calculation of final *R* indices. In the final stage of least-squares refinement, all non-hydrogen atoms were refined anisotropically.

■ ASSOCIATED CONTENT

Ⓢ Supporting Information

This includes crystallographic data for the structures of **3**, **5**, **8**, **16**, and **17**. Tables of crystallographic information (Tables S1−S10) and perspective drawings of the complex cations of **5**, **8**, and **16** (Figures S1−S3). This material is available free of charge via the Internet at http://pubs.acs.org.

■ AUTHOR INFORMATION

Corresponding Author

*E-mail: wwyam@hku.hk. Phone: +(852) 2859-2153. Fax: +(852) 2857-1586.

Notes

The authors declare no competing financial interest.

■ ACKNOWLEDGMENTS

V.W.-W.Y. acknowledges support from the University Grants Committee Areas of Excellence Scheme (AoE/P-03/08) and General Research Fund (GRF) grant from the Research Grants Council of Hong Kong Special Administrative Region, P. R. China (HKU 7063/10P). This work has been supported by the ANR-RGC Joint Research Scheme sponsored by the Research Grants Council of Hong Kong and the French National Research Agency (*Agence Nationale de la Recherche*, ANR) (A-HKU 704/12). E.C.-C.C. acknowledges the receipt of a University Postdoctoral Fellowship; W.-Y.L. and T.K.-M.L. acknowledge the receipt of postgraduate studentships, all from The University of Hong Kong.

■ REFERENCES

(1) (a) *Sulfur: Its Significance for Chemistry, for the Geo-, Bio-, and Cosmosphere and Technology;* Muller, A., Krebs, B., Eds.; Elsevier: Amsterdam, 1984; p 141. (b) Dance, I.; Fisher, K. Metal Chalcogenide Cluster Chemistry. In *Progress in Inorganic Chemistry;* Wiley: Hoboken, NJ, 1994; Vol. 41.

(2) (a) Schmid, G. *J. Chem. Soc., Dalton Trans.* **1998**, 1077. (b) Schmid, G.; Bäumle, M.; Geerkens, M.; Heim, I.; Osemann, C.; Sawitowski, T. *Chem. Soc. Rev.* **1999**, *28*, 179. (c) Green, M.; O'Brien, P. *Chem. Commun.* **1999**, 2235.

(3) (a) Deveson, A.; Dehnen, S.; Fenske, D. *J. Chem. Soc., Dalton Trans.* **1997**, 4491. (b) Corrigan, J. F.; Fenske, D. *Angew. Chem., Int. Ed. Engl.* **1997**, *36*, 1981. (c) Corrigan, J. F.; Fenske, D.; Power, W. P. *Angew. Chem., Int. Ed. Engl.* **1997**, *36*, 1176. (d) Wang, C.-R.; Lo, K. K.-W.; Yam, V. W.-W. *J. Chem. Soc., Dalton Trans.* **1996**, 227. (e) Wang, C.-R.; Lo, K. K.-W.; Yam, V. W.-W. *Chem. Phys. Lett.* **1997**, *262*, 91. (f) Wang, C.-R.; Lo, K. K.-W.; Fung, W. K.-M.; Yam, V. W.-W. *Chem. Phys. Lett.* **1998**, *296*, 505. (g) Yam, V. W.-W.; Lo, K. K.-W. *Comments Inorg. Chem* **1997**, *19*, 209.

(4) (a) Gimeno, M. C.; Laguna, A. *Chem. Soc. Rev.* **2008**, *37*, 1952. (b) Schmidbaur, H.; Schier, A. *Chem. Soc. Rev.* **2008**, *37*, 1931; (c) Yam, V. W.-W.; Lo, K. K.-W. *Chem. Soc. Rev.* **1999**, *28*, 323. (d) Yam, V. W.-W.; Cheng, E. C.-C. *Angew. Chem., Int. Ed. Engl.* **2000**, *39*, 4240. (e) Yam, V. W.-W.; Cheng, E. C.-C. *Chem. Soc. Rev.* **2008**, *37*, 1806.

(5) See, for example: (a) Schmidbaur, H.; Hofreiter, S.; Paul, M. *Nature* **1995**, *377*, 503. (b) Canales, F.; Gimeno, M. C.; Jones, P. G.; Laguna, A. *Angew. Chem., Int. Ed. Engl.* **1994**, *33*, 769. (c) Canales, S.; Crespo, O.; Gimeno, M. C.; Jones, P. G.; Laguna, A. *Chem. Commun.* **1999**, 679. (d) Lensch, C.; Jones, P. G.; Sheldrick, G. M. *Z. Naturforsch., B* **1982**, *37*, 944. (e) Jones, P. G.; Thöne, C. *Chem. Ber.* **1991**, *124*, 2725. (f) Ramamoorthy, V.; Wu, Z.; Yi, Y.; Sharp, P. R. *J. Am. Chem. Soc.* **1992**, *114*, 1526. (g) Yi, Y.; Ramamoorthy, V.; Sharp, P. R. *Inorg. Chem.* **1993**, *32*, 1946.

(6) (a) Pyykkö, P. *Chem. Rev.* **1997**, *97*, 597. (b) Bates, P. A.; Waters, J. M. *Acta Crystallogr., Sect. A* **1987**, *43*, C194. (c) Hofreiter, S.; Paul, M.; Schmidbaur, H. *Chem. Ber.* **1995**, *128*, 901. (d) Canales, F.; Gimeno, M. C.; Laguna, A.; Jones, P. G. *J. Am. Chem. Soc.* **1996**, *118*, 4839. (e) Canales, S.; Crespo, O.; Gimeno, M. C.; Jones, P. G.; Laguna, A.; Mendizabal, F. *Organometallics* **2000**, *19*, 4985. (f) Fenske, D.; Langetepe, T.; Kappes, M. M.; Hampe, O.; Weis, P. *Angew. Chem., Int. Ed.* **2000**, *39*, 1857.

(7) (a) Yam, V. W.-W.; Cheng, E. C.-C.; Cheung, K.-K. *Angew. Chem., Int. Ed. Engl.* **1999**, *38*, 197. (b) Yam, V. W.-W.; Cheng, E. C.-C.; Zhou, Z.-Y. *Angew. Chem., Int. Ed. Engl.* **2000**, *39*, 1683. (c) Yam,

V. W.-W.; Cheng, E. C.-C.; Zhu, N. *Angew. Chem., Int. Ed. Engl.* **2001**, *40*, 1763. (d) Lebedkin, S.; Langetepe, T.; Sevillano, P.; Fenske, D.; Kappes, M. M. *J. Phys. Chem. B.* **2002**, *106*, 9019. (e) Lee, T. K.-M.; Zhu, N.; Yam, V. W.-W. *J. Am. Chem. Soc.* **2010**, *132*, 17646. (f) Yam, V. W.-W.; Cheng, E. C.-C. *Top. Curr. Chem.* **2007**, *281*, 269. (g) Chapter 19. In *Nanoscale Phenomena;* Tang, Z., Sheng, P., Eds.; Springer: New York, 2008.

(8) (a) He, X.; Cheng, E. C.-C.; Zhu, N.; Yam, V. W.-W. *Chem. Commun.* **2009**, 4016. (b) He, X.; Lam, W. H.; Zhu, N.; Yam, V. W.-W. *Chem.—Eur. J.* **2009**, *15*, 8842. (c) Hau, F. K.-W.; He, X.; Lam, W. H.; Yam, V. W.-W. *Chem. Commun.* **2011**, *47*, 8778. (d) Koshevoy, I. O.; Chang, Y. C.; Karttunen, A. J.; Selivanov, S. I.; Jänis, J.; Haukka, M.; Pakkanen, T.; Tunik, S. P.; Chou, P. T. *Inorg Chem.* **2012**, *51*, 7392.

(9) (a) Wang, Q.-M.; Lee, Y.-A.; Crespo, O.; Deaton, J.; Tang, C.; Gysling, H. J.; Gimeno, M. C.; Larraz, C.; Villacampa, M. D.; Laguna, A.; Eisenberg, R. *J. Am. Chem. Soc.* **2004**, *126*, 9488. (b) Jia, J.-H.; Wang, Q.-M. *J. Am. Chem. Soc.* **2009**, *131*, 16634.

(10) (a) Corrigan, J. F.; Fenske, D. *Chem. Commun.* **1996**, 943. (b) Fenske, D.; Ohmer, J.; Hachgenei, J.; Merzweiler, K. *Angew. Chem., Int. Ed.* **1998**, *27*, 1277.

(11) Jones, P. G.; Lensch, C.; Sheldrick, G. M. *Z. Naturforsch., B* **1982**, *37*, 141.

(12) (a) Marbach, G.; Strähle, J. *Angew. Chem., Int. Ed. Engl.* **1984**, *23*, 715. (b) Huang, S.-P.; Kanatzidis, M. G. *Angew. Chem., Int. Ed. Engl.* **1992**, *31*, 787. (c) Vicente, J.; Chicote, M. T.; González-Herrero, P.; Grünwald, C. *Organometallics* **1997**, *16*, 3381.

(13) (a) Balakrishna, M. S.; Reddy, V. S.; Krishnamurthy, S. S. *Coord. Chem. Rev.* **1994**, *129*, 1. (b) Yam, V. W.-W.; Chan, C.-L.; Cheung, K.-K. *J. Chem. Soc., Dalton Trans.* **1996**, 4019.

(14) (a) Kyle, K. R.; Ryu, C. K.; DiBenedetto, J. A.; Ford, P. C. *J. Am. Chem. Soc.* **1991**, *113*, 2954. (b) Ford, P. C.; Cariati, E.; Bourassa, J. *Chem. Rev.* **1999**, *99*, 3625. (c) Hao, L.; Mansour, M. A.; Lachicotte, R. J.; Gysling, H. J.; Eisenberg, R. *Inorg. Chem.* **2000**, *39*, 5520.

(15) Hermolin, J.; Levin, M.; Kosower, E. M. *J. Am. Chem. Soc.* **1981**, *103*, 4808.

(16) (a) Wiegräbe, W.; Bock, H. *Chem. Ber.* **1968**, *101*, 1414. (b) Cross, R. J.; Green, T. H.; Keat, R. *J. Chem. Soc., Dalton Trans.* **1976**, 1424. (c) Ellermann, J.; Mader, L. *Spectrochim. Acta* **1981**, *37A*, 449.

(17) (a) Schmidbaur, H.; Wagner, F. E.; Wohlleben-Hammer, A. *Chem. Ber.* **1979**, *112*, 496. (b) Yam, V. W.-W.; Choi, S. W.-K. *J. Chem. Soc., Dalton Trans.* **1994**, 2057.

(18) Otwinowski, Z., Minor, W., Gewirth, D. *DENZO,* Version 1.3.0 with *The HKL Manual—A Description of Programs DENZO, XDISPLAYF, and SCALEPACK*; Yale University: New Haven, CT, 1995.

(19) Sheldrick, G. M. *SHELXS 97: Programs for Crystal Structure Analysis (release 97–2);* University of Göttingen: Göttingen, Germany, 1997.